Catalysis Today 166 (2011) 188–193

Contents lists available at ScienceDirect

Catalysis Today

journal homepage: www.elsevier.com/locate/cattod

Selective catalytic reduction of NO by CO over CuO supported on SBA-15: Effect of CuO loading on the activity of catalysts

Archana Patel, Thomas E. Rufford, Victor Rudolph, Zhonghua Zhu*

School of Chemical Engineering, The University of Queensland, St. Lucia, Brisbane, 4072 QLD, Australia

ARTICLE INFO

Article history:
Available online 10 July 2010

Keywords:
Nitric oxide
Selective catalytic reduction
Mesoporous silica
SBA-15
Copper oxide

ABSTRACT

CuO supported on mesoporous silica SBA-15 was investigated as a catalyst for selective catalytic reduction of NO by CO. The CuO/SBA-15 catalysts were prepared by wet impregnation with copper loadings of 4.01–10.1 wt%. The catalysts were characterized by N_2 adsorption, XRD, ICP, H_2-temperature programmed reduction (TPR) and NO-temperature programmed desorption. The most active CuO/SBA-15 catalyst in this study was Cat-B, containing 8.67 wt% Cu on silica. This catalyst achieved 60% NO reduction in catalytic tests. Increasing the Cu loading to 10.1 wt% resulted in a less active catalyst (Cat-C) than for Cu loadings less than 10 wt%. The reduced activity of Cat-C for the NO + CO reaction was attributed to formation of bulk CuO aggregates on the SBA-15 particles and a Cu_2O phase at high Cu loadings, as confirmed by TPR experiments and XRD measurements.

1. Introduction

Nitric oxides (NO_x) and carbon monoxide (CO) are hazardous pollutants emitted from the combustion of fossil fuels in coal-fired power stations and in automobiles. NO is a greenhouse gas and contributes to other environmental problems such as acid rain and smog. NO_x and CO pollution can also have negative impacts on human health, with effects on asthma, emphysema, bronchitis, and heart diseases [1]. The commercial technology for post-combustion NO_x control in coal-fired electricity generation plants, which account for 53% of total NO_x emissions [2], is selective catalytic reduction (SCR) using ammonia or urea as reducing agents. The high process and materials handling costs of using ammonia or urea for SCR of NO may be overcome by choosing an alternative reducing agent, such as carbon monoxide or light hydrocarbons. Supported noble metals like Rh/TiO_2 [3], Au/CeO_2 [4,5], Ag/CeO_2 [6] and Ag/TiO_2 [7], Pd/CeO_2 [8], and Pd on perosvkite and alumina modified silica [9,10], have been widely studied as catalysts for NO reduction by CO. Although noble metal catalysts show good activity for this reaction at low temperatures, application of noble metal SCR in power plants is cost prohibitive.

Metal oxide catalysts, including NiO, CuO and MnO_x, on various support materials (titania, alumina, silica, or zirconia) have been studied for NO_x reduction by CO [9–12]. CuO catalysts are among the most promising of these non-noble metal catalysts for NO reduction by CO at 200–550 °C [13–17]. Early studies by Iwamoto et al. [18] on CuO catalysts for NO_x SCR reported Cu^{2+} ion-exchanged zeolites with good activity for NO reduction, however, recent studies have highlighted that although Cu^{2+} ion-exchanged zeolites show good activity for NO reduction these catalyst suffer from poor hydrothermal stability and deactivation by sintering of Cu^{2+} to large CuO at high temperatures [18–21]. In efforts to stabilise the active copper phases, researchers have studied mesoporous support materials as hosts for nanosized CuO catalyst particles.

Mesoporous materials have proven to be useful catalyst supports because the mesopores provide large specific surface areas and large pore volumes for achieving high catalyst metal loadings and well dispersed metal deposition. Additionally, many synthesis techniques for mesoporous materials produce uniform pore sizes and ordered pore structures, which can both be advantageous for catalyst studies [22]. Factors affecting the dispersion of CuO catalyst particles on mesoporous supports include the catalyst preparation method, the amount of copper loaded, and the pore structure of the support. In an example highlighting the effect of pore structure on CuO dispersion, better CuO dispersion was reported using the a mesoporous ZSM-11 zeolite with straight channels than when CuO was loaded on a mesoporous ZSM-5, which had both straight and sinusoidal channels [23]. The Cu-ZSM-11 catalyst was reported to be twice as active for direct NO decomposition as the Cu-ZSM-5. As well as pore structure, the acidity of the support influences the catalyst activity. Support materials with lower acidity, such as silica modified with titania, can produce a homogeneous CuO phase compared to heterogeneous CuO phases on a more acidic support. The CuO catalysts on the less acidic supports were reported to have higher activity for NO reduction by hydrocarbons [24–28].

* Corresponding author. Tel.: +61 7 3365 3528; fax: +61 3365 4199.
E-mail address: z.zhu@uq.edu.au (Z. Zhu).

0920-5861/$ – see front matter © 2010 Elsevier B.V. All rights reserved.
doi:10.1016/j.cattod.2010.05.040

Catalyst loading by wet impregnation has been reported to produce homogeneous dispersions of small metal particles within silica mesopores, without affecting the mesoporous structure [29–33]. The small CuO particles can then be reduced at lower temperatures compared to bulk CuO particles. The choice of copper precursor can also influence the activity of the CuO-based catalysts, as the strength of interaction between the copper precursor and the support will influence the dispersion of the metal. For example, catalyst impregnation by an aqueous or organic copper precursor resulted in catalysts with different concentrations of Cu^{2+} sites on MCM-41 and MCM-48 supports [22].

In our current study of CuO catalysts for SCR of NO by CO ($NO + CO \rightarrow 1/2\ N_2 + CO_2$), we selected the ordered mesoporous silica (SBA-15) with straight pore channels, as the catalyst support. CuO is a good candidate catalyst for the NO + CO reaction as it can directly reduce NO and also oxidize CO. We report here the effect of copper loading on the dispersion of CuO on SBA-15 and subsequent impacts on the activity of the CuO/SBA-15 catalysts for NO reduction by CO.

2. Materials and methods

2.1. Catalyst preparation and characterization

Mesoporous silica SBA-15 was prepared according to the method described by Zhao et al. [34]. 12 g of Pluronic P123 triblock copolymer and 13.44 g of potassium chloride were dissolved in 360 ml of 32% hydrochloric acid by stirring for 2 h. Then 24.96 g of tetraethyl orthosilicate (TEOS) was added and the solution was aged for 24 h at 40 °C. The resulting sol was transferred to a Teflon lined autoclave and hydrothermally treated at 100 °C for 24 h. The white precipitate was filtered, rinsed with water and dried at room temperature for 24 h. The white powder was then calcined at 550 °C for 6 h to obtain mesoporous silica SBA-15.

The CuO/SBA-15 catalysts were prepared by wet impregnation. The SBA-15 was impregnated with aqueous solutions containing the desired amount of $Cu(NO_3)_2{\cdot}3H_2O$ for different CuO loadings. The $Cu(NO_3)_2{\cdot}3H_2O$ impregnated SBA-15 samples were dried overnight, then calcined at 350 °C for 6 h to decompose the $Cu(NO_3)_2$. The copper contents of the catalysts were determined by inductively coupled plasma optical emission spectrometry (ICP-OES, Varian Vista Pro). Catalysts were prepared containing 4.02 wt%, 8.67 wt%, and 10.1 wt% copper on SBA-15. These three samples are referred to as Cat-A, Cat-B and Cat-C.

X-ray diffraction (XRD) patterns of the SBA-15 and CuO/SBA-15 catalysts were collected on two instruments. Small angle XRD was performed in the range of $2\theta = 0.5–6°$ using a Bruker D8 Advanced Research diffractometer with a Cu-Kα radiation source at 40 kV and 30 mA. To identify copper and copper oxide phases present in the catalysts, powder XRD over a wider angle range was also performed using a Rigaku Miniflex diffractometer with a Cu Kα radiation source.

N_2 adsorption–desorption isotherms were measured at −196 °C, after degassing samples for 24 h at 200 °C, on a Quadrasorb *SI* (Quantachrome). Specific surface areas (S_{BET}) of the SBA-15 and CuO/SBA-15 catalysts were calculated by the Brunauer–Emmett–Teller (BET) equation. Total pore volumes (V_p) were evaluated at relative pressures (P/P_0) close to unity. Pore size distributions were calculated by using non-local density function theory (DFT) for cylindrical silica pores (algorithm supplied in the Quadrawin software package).

2.2. Temperature programmed reduction and NO-desorption measurements

Temperature programmed reduction (TPR) of the CuO/SBA-15 catalysts in H_2 was studied with a Belcat instrument. Typically 50 mg of catalyst was loaded, along with quartz wool, into a U-shaped quartz cell (i.d. 9 mm). Prior to TPR the catalyst was heated *in situ* at 350 °C for 1 h in a flow of He. Reduction was carried out by heating at 10 °C min^{-1} from room temperature to 900 °C in 5% H_2 in He flowing at 30 mL min^{-1}. H_2 consumption was measured continuously with a thermal conductivity detector. Water produced during TPR was trapped in a zeolite column upstream of the detector.

Temperature programmed desorption (TPD) of NO was measured after pre-treatment of the catalyst in a similar method to that described for TPR. The NO adsorption step was performed at 30 °C by passing 50 mL min^{-1} of 0.1% NO in He over the catalyst for 2 h. The catalyst was then flushed with 30 mL min^{-1} of He to remove any physically adsorbed species. TPD was performed from 30 °C to 500 °C at a heating rate of 10 °C min^{-1} using He as the carrier gas.

2.3. Evaluation of catalyst activity

The catalytic experiments for the NO + CO reaction were conducted with 0.1 g of catalyst in a vertical quartz tube reactor (i.d. 9 mm). The catalyst was first heated in Ar at 300 °C for 1 h. Then the reactor temperature was adjusted to the desired reaction temperature and the gas feed was switched from Ar to a mixture of 500 ppm NO and 500 ppm CO in He. A total reactor flow rate of 80 mL min^{-1} was selected to ensure the reaction rate was not limited by external diffusion. The reaction was studied in the temperature range of 350–550 °C. NO concentrations at the reactor inlet (NO_{in}) and reactor outlet (NO_{out}) were measured using a chemiluminescence NO_x analyser (Thermo 42i). This analyser also measures the concentration of NO_2 in a gas stream and no NO_2 was detected in the reactor feed gas. The conversion of NO (X_{NO}) was calculated using Eq. (1):

$$X_{NO} = \frac{(NO_{in} - NO_{out})}{NO_{in}} \quad (1)$$

The catalyst was left to stabilise for 30 min at each temperature before the NO concentration at the reactor outlet was noted for the conversion calculation.

3. Results and discussion

3.1. Physical characterization of CuO/SBA-15 catalysts

In Fig. 1 the small angle XRD pattern of SBA 15 shows defined peaks between 1° and 2.5°, which confirm the 2D hexagonal *p6mm* structure of SBA-15 [34]. The powder XRD pattern of SBA-15 in Fig. 2 shows the presence of an amorphous silica phase, with a broad diffraction observed around $2\theta = 24°$ (JCPDS 13-0026, 51-1592 and 56-0505). The diffraction patterns of the CuO/SBA-15 catalysts are also presented in Fig. 2. For the CuO/SBA-15 catalysts the sharp diffraction peaks at $2\theta = 42°$, 46° and 75° identify a crystalline CuO phase. The intensities of these CuO peaks increase with increasing CuO loading. The catalyst containing 10.1 wt% Cu (Cat-C) exhibits an additional peak at $2\theta = 65°$, which can be attributed to a Cu_2O phase (JCPDS no. 78-2076).

The N_2 adsorption–desorption isotherm for SBA-15, shown in Fig. 3, presents a Type IV isotherm (IUPAC classification) with a H1 hysteresis. This type of hysteresis between relative pressures of 0.6–0.8 is indicative of capillary condensation within cylindrical mesopores [35]. The sharp steps in the adsorption and desorption isotherms indicate a narrow pore size distribution, as shown by the DFT pore size distribution plot. The DFT results in Fig. 3 show that the peak pore radius in the SBA-15 is around 40 Å, with a second distribution of pores with radius 10–15 Å.

Fig. 4 shows (a) N_2 adsorption–desorption isotherms and (b) DFT pore size distributions of the CuO/SBA-15 catalysts. Like the pristine SBA-15, all three CuO impregnated SBA-15 samples exhibit Type IV

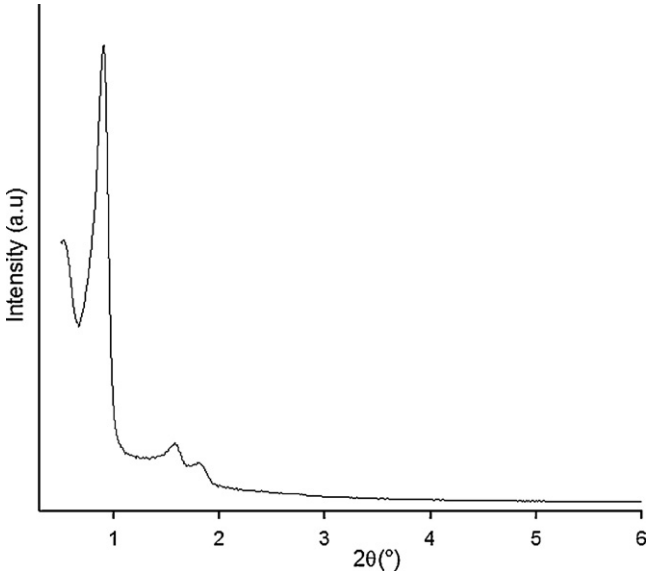

Fig. 1. Small angle X-ray diffraction pattern of mesoporous silica SBA-15.

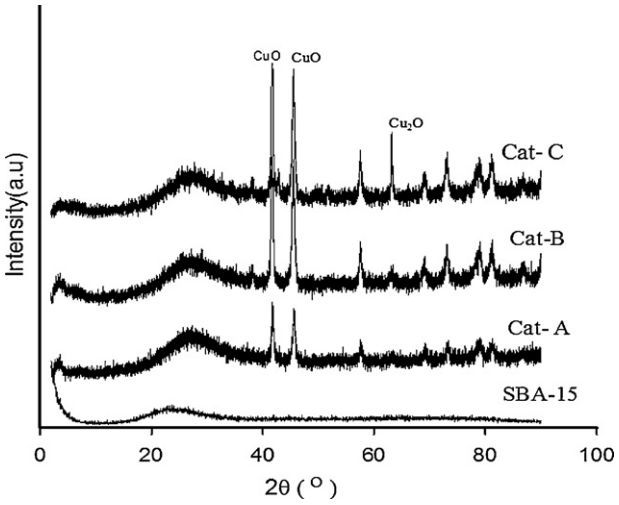

Fig. 2. Powder X-ray diffraction pattern of SBA-15 silica and CuO/SBA-15 catalysts with Cu loadings of 4.01 wt% (Cat-A), 8.67 wt% (Cat-B) and 10.1 wt% (Cat-C).

isotherms with defined adsorption and desorption isotherm steps observed between relative pressures of 0.6–0.8. The isotherm steps and hysteresis loops indicate that the CuO/SBA-15 catalysts retain the mesoporosity of the SBA-15 support. The CuO/SBA-15 catalysts adsorbed less N_2 than the pristine SBA-15; however, the total pore volume and specific surface areas did not show a linear decrease with increasing CuO loading from 4.01 wt% to 10.1 wt% (see Table 1). The surface area and pore volume of the Cat-C was higher than the two catalysts with lower Cu loadings. This unexpected result may be due to blockage of SBA-15 pore openings by $Cu(NO_3)_2{\cdot}3H_2O$ at and deposition of CuO particles on the external surface of the SBA-15 particles high copper loadings.

The pore size distributions (Fig. 4b) of CuO/SBA-15 catalysts provide indication about where the CuO has been deposited on the

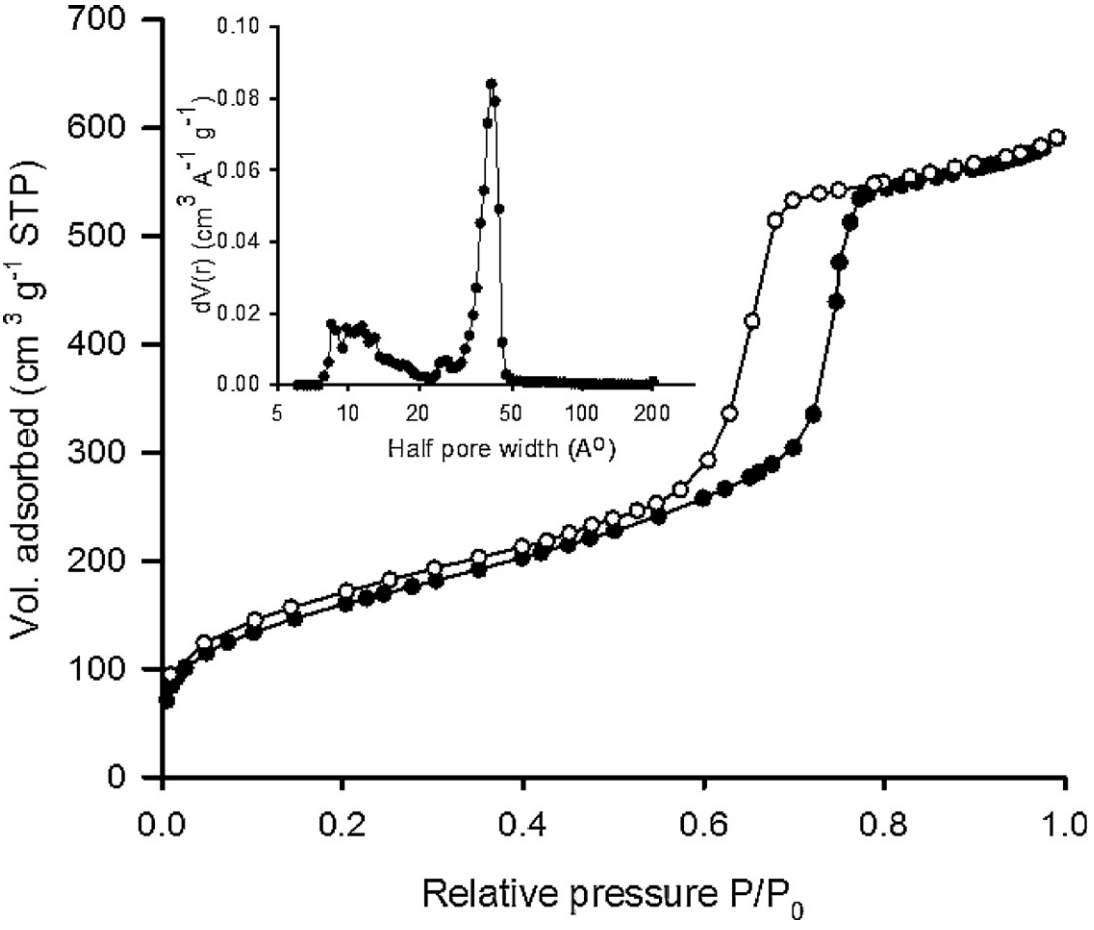

Fig. 3. N_2 adsorption–desorption isotherms on SBA-15 silica at −196 °C, (● adsorption isotherm, ○ desorption isotherm). Inset: DFT pore size distribution.

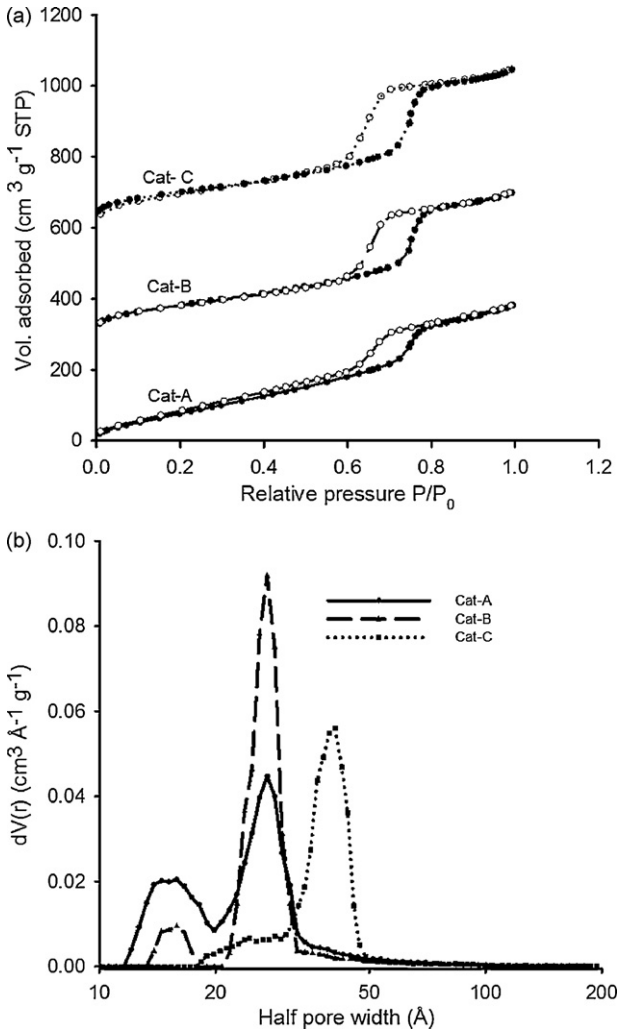

Fig. 4. (a) N_2 adsorption–desorption isotherms at −196 °C on CuO/SBA-15 catalysts with Cu loadings of 4.01 wt% (Cat-A), 8.67 wt% (Cat-B) and 10.1 wt% (Cat-C) (● adsorption isotherm, ○ desorption isotherm). (b) DFT pore size distributions.

SBA-15 support. For Cu loadings of 4.01 wt% and 8.67 wt%, Fig. 4b shows that the 40 Å radius pores of SBA-15 are partially filled by CuO shifting the peak in the pore size distributions to around 30 Å. The smaller pores of SBA-15 at 10–15 nm are also partially filled, with greater volume of these pores filled for Cat-B than Cat-A. The SBA-15 peak pore radius at 40 Å is retained for Cat-C, which suggests that copper was not deposited in the 40 Å channels at high Cu loading.

3.2. Temperature programmed desorption of NO on CuO/SBA-15 catalysts

The TPD profiles of NO from the CuO/SBA-15 catalysts are presented in Fig. 5. For all three catalysts, desorption peaks are observed at 90–110 °C. This low temperature desorption could include both desorption of NO and desorption of N_2O from the catalyst, although the thermal conductivity detector cannot distinguish the different species. At 90–110 °C desorption of NO would be from copper (II) sites of CuO, while the N_2O can result from breaking of Cu–NO bonds. A second desorption peak is observed at 300 °C for Cat-B. This high temperature peak could be attributed to desorption of NO from a bidentsate surface nitrate species [36].

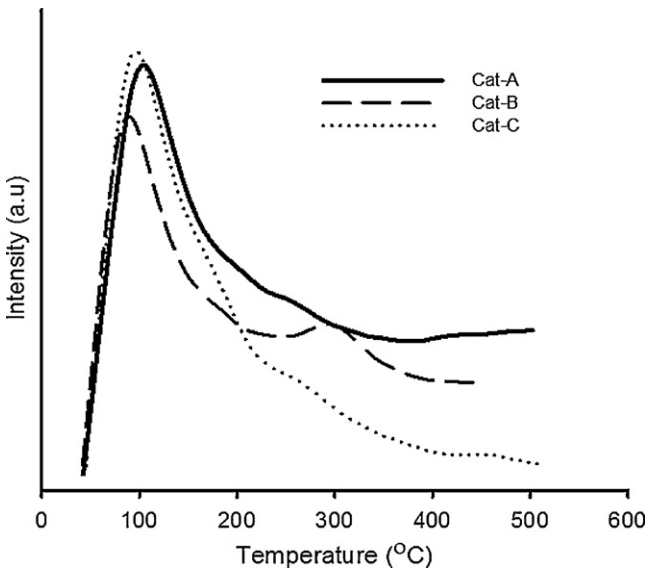

Fig. 5. NO-Temperature programmed desorption profiles of CuO/SBA-15 catalysts with Cu loadings of 4.01 wt% (Cat-A), 8.67 wt% (Cat-B) and 10.1 wt% (Cat-C).

3.3. Temperature programmed reduction of CuO/SBA-15 catalysts

Fig. 6 shows TPR profiles of CuO/SBA-15 catalysts reduced with H_2. The reduction of CuO particles to Cu metal was confirmed in all three samples. For Cat-A a broad H_2 consumption peak is observed in the temperature range of 170–400 °C. For Cat-B two reduction peaks are observed at 270 °C and 370 °C, respectively. H_2 consumption below 300 °C is attributed to the reduction of highly dispersed Cu^{2+} in small CuO particles and bulk CuO to Cu^{1+} [37–39]. The high temperature H_2 consumption peak at 370 °C observed for Cat-B may result from the direct reduction of aggregated CuO particles to Cu metal [40].

The reducibility of the CuO/SBA-15 catalysts is summarised in Table 2. The highest H_2 consumption was observed for Cat-B and this sample had the greatest degree of CuO reduction, based on the Cu content and H_2 consumption. The almost complete reduction of CuO to Cu metal in Cat-B, combined with XRD data, suggests that at a Cu loading of 8.67 wt% the CuO species are well dispersed [40]. More than 90% of the CuO was also reduced in Cat-A. At lower Cu loadings, there are more isolated Cu^{2+} species with strong support interactions than there are in Cat-B. These isolated Cu^{2+} species are more difficult to reduce than small CuO particles [40].

Cat-C was more difficult to reduce than Cat-A or Cat-B, and required higher temperatures for reduction. For Cat-C the peaks in

Table 1
Textural properties of SBA-15 and CuO/SBA-15 catalysts.

Sample	S_{BET} ($m^2\ g^{-1}$)	V_p ($cm^3\ g^{-1}$)	Cu loading (wt%)
SBA-15	574	1.032	–
Cat-A	355	0.55	4.02
Cat-B	320	0.6	8.67
Cat-C	368	0.75	10.1

Table 2
H_2 consumption and amount of CuO reduced for CuO/SBA15 with CuO loading of 4.01 wt% (Cat-A), 8.67 wt% (Cat-B) and 10.1 wt% (Cat-C).

Sample	Temperature of peak maximum (°C)		Total H_2 consumption (mmol g^{-1} catalyst)	CuO reduced (%)
	First peak	Second peak		
Cat-A	245	–	0.918	91.3
Cat-B	280	365	2.150	99.2
Cat-C	380	530	1.459	57.0

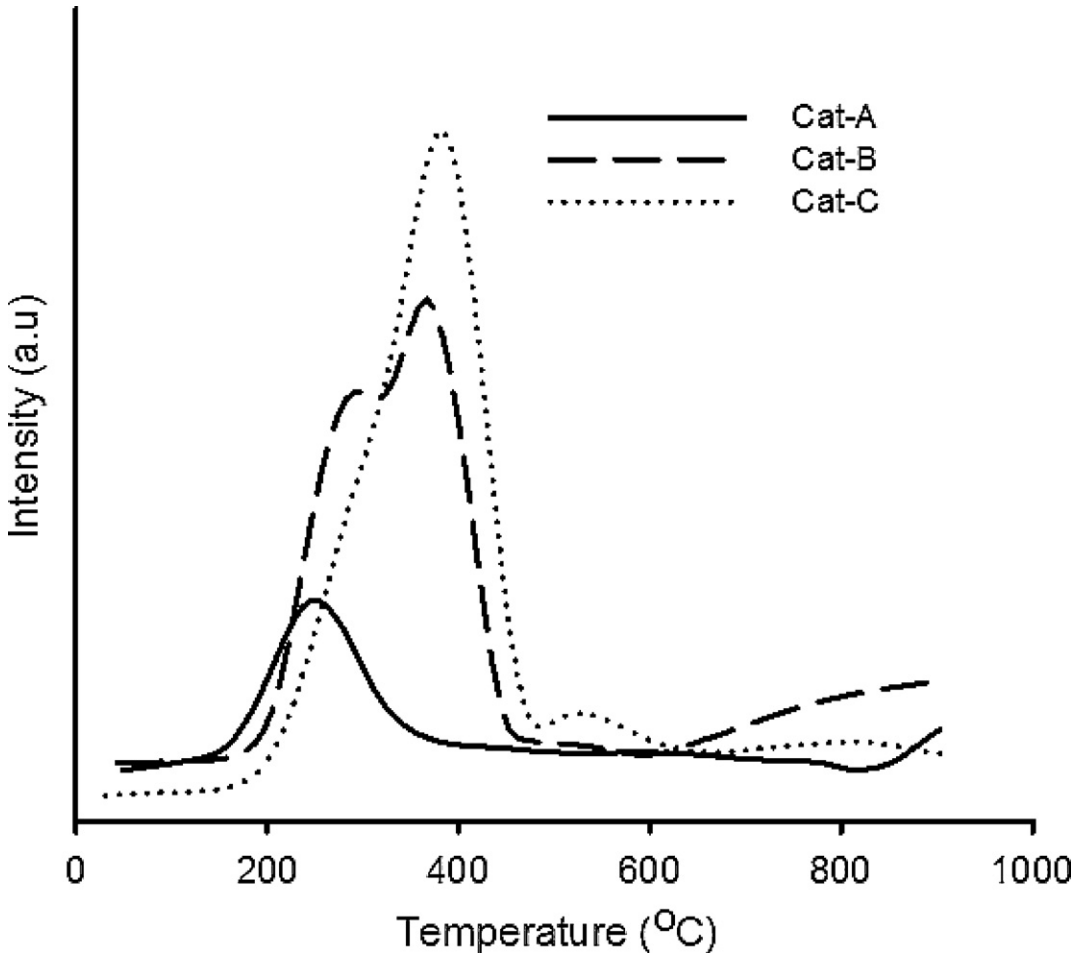

Fig. 6. H_2-Temperature programmed reduction profiles of CuO/SBA-15 catalysts with Cu loadings of 4.01 wt% (Cat-A), 8.67 wt% (Cat-B) and 10.1 wt% (Cat-C).

H_2 consumption were recorded at 370 °C and from 450 °C to 600 °C. The reduction observed above 450 °C may be associated with reduction of Cu^{1+} of the Cu_2O phase to Cu metal [37–39]. The 370 °C peak indicates reduction of CuO to Cu^{1+}, as observed at lower temperatures for Cat-A and Cat-B. The higher temperature for CuO reduction in Cat-C indicates that this sample contains bulk or aggregate CuO particles that are larger than those found in the catalyst prepared with less than 10 wt% Cu.

3.4. Activity of CuO/SBA-15 in NO reduction

The conversion of NO by CO was found to increase with reaction temperature for all three CuO/SBA-15 catalysts, as shown in Fig. 7. For each catalyst and all reaction conditions there was no NO_2 recorded by the chemiluminescence NO_x analyser, which confirms the selective reduction of NO to N_2. For all three CuO/SBA-15 catalysts the conversion of NO at 300 °C is less than 20% (at GHSV = 48,000 L^{-1} h^{-1} kg^{-1}), which is lower than NO conversion reported for SCR with strong reducing agents, such as SCR with NH_3 over CuO/Al_2O_3 catalysts (GHSV = 14,000 L^{-1} h^{-1} kg^{-1}) [41] or SCR with C_3H_6 over Cu-Al-MCM-41 (GHSV = 60,000 L^{-1} h^{-1} kg^{-1}) [40]. At high temperatures (above 400 °C) CuO/SBA-15 catalysts Cat-A and Cat-B show increased and sustained activity to convert up to 60% of NO. At temperatures of 400–450 °C the rate of conversion of NO by CO observed for CuO/SBA-15 is comparable to some reports of SCR by NH_3 over copper based catalysts [41], and although lower reaction temperatures may be desired in NO reduction technologies

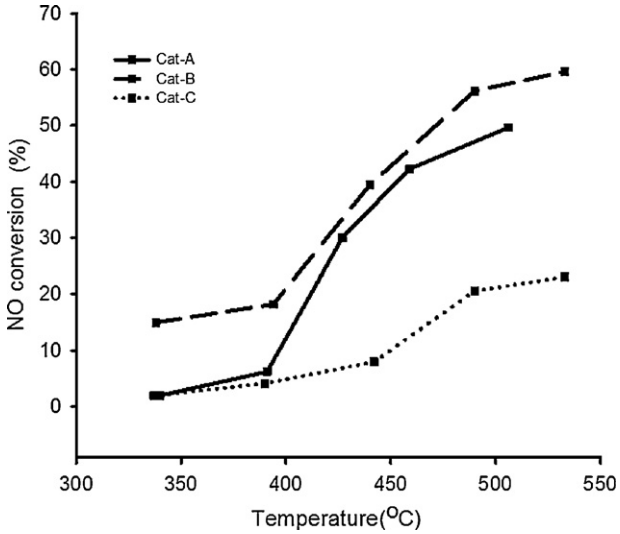

Fig. 7. Profiles of NO conversion as a function of reaction temperature of CuO/SBA-15 catalysts with Cu loadings of 4.01 wt% (Cat-A), 8.67 wt% (Cat-B) and 10.1 wt% (Cat-C). Reactor conditions: total flow rate: 80 ml/min, NO_{in}: 500 ppm, CO_{in}: 500 ppm.

the SCR without NH_3 or hydrocarbon injection offers processing advantages.

The activity of the CuO/SBA-15 catalysts for NO reduction increased with the increase in Cu loading from 4.01 wt% to 8.67 wt%

(Fig. 7), however, lower NO conversion was observed when the Cu loading was increased to 10.1 wt%. As shown by the activity curves for Cat-A and Cat-B, the positive effect of increasing Cu loading was more pronounced at temperatures below 400 °C. The high activity of Cat-B results from the well dispersed, small CuO particles in this sample [40]. The catalytic results are consistent with the TPR and TPD results, in which Cat-B was both the easiest catalyst to reduce and the catalyst that had the strongest interaction with NO. The highly dispersed CuO particles in Cat B are more active than the bulk CuO and Cu_2O [43] observed in Cat-C, and more active than the isolated Cu^{2+} species with strong support interactions that may be present in Cat-A.

In this study copper catalysts supported on mesoporous silica have shown activity for the reduction of NO by CO. In a real flue gas application these catalysts will be affected by contaminants such as H_2O and SO_2, both contaminants can inhibit NO reduction or lead to catalyst deactivation [42]. We intend to investigate the stability of CuO supported on mesoporous silicas under oxidizing conditions – including SO_2 – in our future experiments.

4. Conclusions

CuO supported on mesoporous silica SBA-15 is active for selective catalytic reduction of NO by CO. The conversion of NO over CuO/SBA-15 catalysts increases for catalyst Cu content up to 8.67 wt%. At higher Cu loadings the activity of CuO/SBA-15 falls due to an increase in CuO particle size and the formation of Cu_2O phases. In this study the catalyst containing 8.67 wt% Cu was the most active catalyst for NO conversion. The superior activity of this catalyst is due to highly dispersed CuO particles in the SBA-15 mesopores. At lower Cu loadings, some isolated Cu^{2+} species with strong support interactions are present (along with dispersed CuO particles). These isolated Cu^{2+} species are both more difficult to reduce in H_2 TPR experiments and less active for the NO + CO reaction than the well dispersed CuO particles.

Acknowledgements

Financial support for this research was provided by the Australian Research Council and Indigo Technologies Pty Ltd. (through ARC Linkage Project LP0775429).

References

[1] S.E. Manahan, Environmental Chemistry, seventh ed., Lewis Publishers, Boca Raton, 2000.
[2] K.B. Schnelle Jr., C.A. Brown (Eds.), Air Pollution Control Technology Handbook, CRC Press, Boca Raton, 2002.
[3] D.I. Kondarides, T. Chafik, X.E. Verykios, J. Catal. 191 (2000) 147–164.
[4] L. Ilieva, G. Pantaleo, I. Ivanov, A.M. Venezia, D. Andreeva, Appl. Catal. B 65 (2006) 101–109.
[5] L. Ilieva, G. Pantaleo, R. Nedyalkova, J.W. Sobczak, W. Lisowski, M. Kantcheva, A.M. Venezia, D. Andreeva, Appl. Catal. B 90 (2009) 286–294.
[6] H. Zhang, A. Zhu, X. Wang, Y. Wang, C. Shi, Catal. Commun. 8 (2007) 612–618.
[7] Z. Liu, J. Li, A.S.M. Junaid, Catal. Today, in press.
[8] S. Roy, M.S. Hegde, Catal. Commun. 9 (2008) 811–815.
[9] J.M. Díaz Cónsul, I. Costilla, C.E. Gigola, I.M. Baibich, Appl. Catal. A 339 (2008) 151–158.
[10] M.S. Khristova, S.P. Petrović, A. Terlecki-Baričević, D.R. Mehandjiev, Central Eur. J. Chem. 7 (2009) 857–863.
[11] Y. Wang, A. Zhu, Y. Zhang, C.T. Au, X. Yang, C. Shi, Appl. Catal. B 81 (2008) 141–149.
[12] Z. Wu, R. Jin, Y. Liu, H. Wang, Catal. Commun. 9 (2008) 2217–2220.
[13] H. Zhu, M. Shen, F. Gao, Y. Kong, L. Dong, Y. Chen, C. Jian, Z. Liu, Catal. Commun. 5 (2004) 453–456.
[14] X.Y. Jiang, G.H. Ding, L.P. Lou, Y.X. Chen, X.M. Zheng, J. Mol. Catal. A: Chem. 218 (2004) 187–195.
[15] J.D.A. Bellido, E.M. Assaf, Fuel 88 (2009) 1673–1679.
[16] Y. Hu, L. Dong, J. Wang, W. Ding, Y. Chen, J. Mol. Catal. A: Chem. 162 (2000) 307–316.
[17] C.C. Pantazis, D.E. Petrakis, P.J. Pomonis, Appl. Catal. B 77 (2007) 66–72.
[18] M. Iwamoto, H. Furukawa, Y. Mine, F. Uemura, S.-i. Mikuriya, S. Kagawa, J. Chem. Soc. Chem. Commun. (1986) 1272–1273.
[19] V. Tomaslic, Z. Gomzi, S. Zrncevic, Appl. Catal. B 18 (1998) 233–240.
[20] K.C.C. Kharas, H.J. Robota, D.J. Liu, Appl. Catal. B 2 (1993) 225–237.
[21] R.A. Grinsted, H.-W. Jen, C.N. Montreuil, M.J. Rokosz, M. Shelef, Zeolites 13 (1993) 602–606.
[22] K. Hadjiivanov, T. Tsoncheva, M. Dimitrov, C. Minchev, H. Knözinger, Appl. Catal. A 241 (2003) 331–340.
[23] M.Y. Kustova, S.B. Rasmussen, A.L. Kustov, C.H. Christensen, Appl. Catal. B 67 (2006) 60–67.
[24] S. Bennici, P. Carniti, A. Gervasini, Catal. Lett. 98 (2004) 187–194.
[25] S. Bennici, A. Gervasini, Appl. Catal. B 62 (2006) 336–344;
S. Bennici, A. Gervasini, M. Lazzarin, V. Ragaini, Ultrason. Sonochem. 12 (2005) 307–312.
[27] P. Carniti, A. Gervasini, V.H. Modica, N. Ravasio, Appl. Catal. B 28 (2000) 175–185.
[28] J.A. Sullivan, Catal. Lett. 79 (2002) 59–62.
[29] F. Ye, Z. Dong, H. Zhang, Catal. Commun. 10 (2009) 2056–2059.
[30] O. Karvana, H. Atakül, Fuel Process Technol. 89 (2008) 908–915.
[31] R. Köhn, M. Fröba, Catal. Today 68 (2001) 227–236.
[32] Y. Li, D. An, Q. Zhang, Y. Wang, J. Phys. Chem. C 112 (2008) 13700–13708.
[33] Y.P. Suna, H.P. Wanga, C.-Y. Penga, T.L. Hsiunga, Y.-M. Sunc, Y.-J. Huangd, Radiat. Phys. Chem. 75 (2006) 1926–1929.
[34] D. Zhao, J. Feng, Q. Huo, N. Melosh, G.H. Fredrickson, B.F. Chmelka, G.D. Stucky, Science 279 (1998) 548–552.
[35] P.I. Ravikovitch, A.V. Neimark, J. Phys. Chem. B 105 (2001) 6817–6823.
[36] M. Shimokawabe, N. Hatakeyama, K. Shimada, K. Tadokora, N. Takezawa, Appl. Catal. A 87 (1992) 205–218.
[37] M. Khristova, B. Ivanov, I. Spassova, T. Spassov, Catal. Lett. 119 (2007) 79–86.
[38] G. Díaz, R. Pérez-Hernández, A. Gómez-Cortés, M. Benaissa, R. Mariscal, J.L.G. Fierro, J. Catal. 187 (1999) 1–14.
[39] J. Sàrkàny, J.L. d'Itri, W.M.H. Sachtler, Catal. Lett. 16 (1992) 241–249.
[40] Y. Wan, J. Ma, Z. Wang, W. Zhou, S. Kaliaguine, J. Catal. 227 (2004) 242–252.
[41] G. Xie, Z. Liu, Z. Zhu, Q. Liu, J. Ge, Z. Huang, J. Catal. 224 (2004) 42–49.
[42] K. Shanmugapriya, H.-S. You, H.-C. Lee, D.R. Park, J.-S. Lee, C.W. Lee, Bull. Korean Chem. Soc. 28 (2007) 1039–1041.
[43] M.H. Kim, I.-S. Nam, Y.G. Kim, Appl. Catal. B 12 (1997) 125–145.